

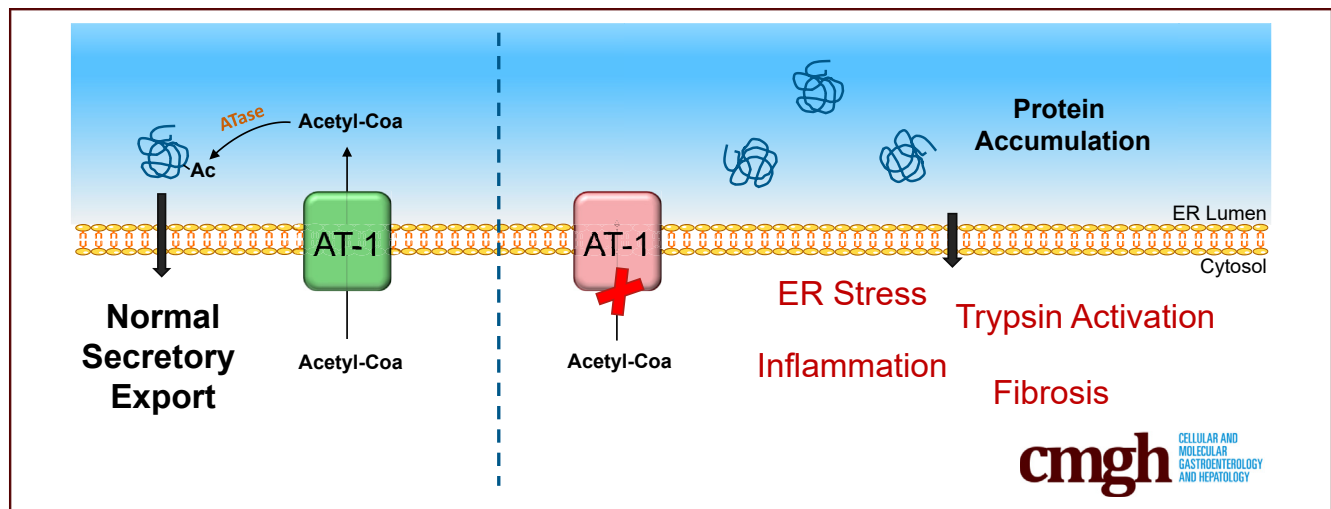
## ORIGINAL RESEARCH

## Deficient Endoplasmic Reticulum Acetyl-CoA Import in Pancreatic Acinar Cells Leads to Chronic Pancreatitis



Michelle M. Cooley,<sup>1</sup> Diana D. H. Thomas,<sup>1</sup> Kali Deans,<sup>1</sup> Yajing Peng,<sup>2</sup> Aurelia Lugea,<sup>3</sup> Stephen J. Pandol,<sup>3</sup> Luigi Puglielli,<sup>2,4</sup> and Guy E. Groblewski<sup>1</sup>

<sup>1</sup>Department of Nutritional Sciences, <sup>2</sup>Department of Medicine, University of Wisconsin-Madison, Madison, Wisconsin; <sup>3</sup>Pancreatic Research Group, Department of Medicine, Cedars-Sinai Medical Center, Los Angeles, California; <sup>4</sup>Geriatric Research Education Clinical Center, Veterans Affairs Medical Center, Madison, Wisconsin



## SUMMARY

Pathologic activation of the unfolded protein response is a key event in the development of pancreatitis. Impairing the endoplasmic reticulum acetyl-CoA transporter AT-1 in acini leads to chronic overactivation of the unfolded protein response and presents a spontaneous chronic pancreatitis phenotype.

**BACKGROUND & AIMS:** Maintaining endoplasmic reticulum (ER) proteostasis is essential for pancreatic acinar cell function. Under conditions of severe ER stress, activation of pathogenic unfolded protein response pathways plays a central role in the development and progression of pancreatitis. Less is known, however, of the consequence of perturbing ER-associated post-translational protein modifications on pancreatic outcomes. Here, we examined the role of the ER acetyl-CoA transporter AT-1 on pancreatic homeostasis.

**METHODS:** We used an AT-1<sup>S113R/+</sup> hypomorphic mouse model, and generated an inducible, acinar-specific, AT-1 knockout mouse model, and performed histologic and biochemical analyses to probe the effect of AT-1 loss on acinar cell physiology.

**RESULTS:** We found that AT-1 expression is down-regulated significantly during both acute and chronic pancreatitis.

Furthermore, acinar-specific deletion of AT-1 in acinar cells induces chronic ER stress marked by activation of both the spliced x-box binding protein 1 and protein kinase R-like ER kinase pathways, leading to spontaneous mild/moderate chronic pancreatitis evidenced by accumulation of intracellular trypsin, immune cell infiltration, and fibrosis. Induction of acute-on-chronic pancreatitis in the AT-1 model led to acinar cell loss and gland atrophy.

**CONCLUSIONS:** These results indicate a key role for AT-1 in pancreatic acinar cell homeostasis, the unfolded protein response, and that perturbations in AT-1 function leads to pancreatic disease. (*Cell Mol Gastroenterol Hepatol* 2021;11:725–738; <https://doi.org/10.1016/j.jcmgh.2020.10.008>)

**Keywords:** AT-1; ER Stress; Unfolded Protein Response.

Pancreatitis is an inflammatory disease of the pancreas that to date lacks specific clinical therapies.<sup>1</sup> The mechanism behind the pathogenesis and progression of pancreatitis involves complex interactions between genetic and environmental factors and thus is not fully understood. One cellular event across nearly all experimental models of both acute pancreatitis (AP) and chronic pancreatitis (CP) is a pathologic activation of the unfolded protein response (UPR), and so remains a key

pathway of interest in the study of exocrine pancreatic disease.<sup>2-4</sup>

The UPR is a well-studied set of cellular pathways designed to monitor and respond to the accumulation of proteins within the endoplasmic reticulum (ER) lumen.<sup>2,4,5</sup> There are 3 protein sensors, in brief: inositol-requiring enzyme 1 (IRE1), which produces a spliced variant of the transcription factor X-box binding protein 1 (XBP1s), activating transcription factor (ATF)6, and protein kinase R-like ER kinase (PERK), which phosphorylates elongation initiation factor 2 $\alpha$  (eIF2 $\alpha$ ). Both XBP1s and ATF6 act to expand the ER and enhance protein folding capabilities, while eIF2 $\alpha$  phosphorylation inhibits cap-dependent protein translation, reducing ER input. If ER stress remains unresolved, PERK signaling increases ATF4, which regulates the expression of the cell death promoter CCAAT/enhancer-binding protein homologous protein (CHOP).

Pancreatic acinar cells are responsible for the production and secretion of digestive enzymes including amylase, pancreatic lipase, and an assortment of inactive protease precursors. Acini show the highest rate of protein synthesis among all mammalian cell types; as such, pancreatic acinar cells rely on a network of mechanisms, including UPR signaling, to maintain ER proteostasis and secretory trafficking.<sup>2,4,6</sup> Previous studies have established essential roles for UPR components in acinar homeostasis and found both protective and pathologic outcomes within the UPR system. For example, the XBP1s protects acinar cells from ethanol-induced damage and acts as an essential factor in exocrine cell differentiation; indeed, homozygous deletion of XBP1 in mice inhibits pancreatic development, while XBP1 heterozygotes are more susceptible to pancreatitis.<sup>7-11</sup> Likewise, PERK-deficient mice show poor exocrine pancreatic development, but deletion of its downstream target CHOP protects against pancreatitis.<sup>12-14</sup>

The UPR is triggered by the aberrant retention of newly synthesized proteins in the ER lumen. Cotranslational and post-translational modifications of nascent proteins in the ER are critical for proper protein folding, stability, and trafficking. In the past decade, a series of studies established the importance of N $\epsilon$ -lysine acetylation for ER proteostasis.<sup>15-17</sup> This process is regulated, in part, by the ER acetyl-CoA transporter AT-1 (also referred to as *SLC33A1*), which moves cytosolic acetyl-CoA into the ER lumen where it is used as a substrate for protein post-translational acetylation by ER-resident acetyltransferases.<sup>18,19</sup> The current hypothesis is that only properly folded proteins in the ER lumen can be acetylated and efficiently trafficked through the secretory pathway, whereas improperly folded proteins are not acetylated and thus are targeted for degradation. Disruption of AT-1 function, as seen with the AT-1 S113R mutation in human beings, manifests as neurodegeneration that is recapitulated in an AT-1<sup>S113R/+</sup> hypomorphic mouse model; these phenotypes are attributed to reductions in secretory efficiency and aberrant induction of ER-associated degradation II/reticulophagy.<sup>20,21</sup> Furthermore, it has been shown recently that loss of AT-1/*SLC33A1* in lung adenocarcinoma cell lines increases the expression of UPR genes and may have effects on ER redox potential.<sup>22</sup> These studies underscore the importance of N $\epsilon$ -lysine acetylation and AT-1 function in the maintenance of

ER proteostasis and cell physiology. However, AT-1 function has yet to be investigated in the context of pancreatic acinar cell function and disease.

Here, we show that AT-1 messenger RNA (mRNA) is up-regulated significantly in the early stages of pancreatitis, and later is down-regulated during experimental AP and CP, suggesting a role for AT-1 in pancreatitis pathophysiology. To that end, we used both the systemic AT-1<sup>S113R/+</sup> hypomorphic mouse model as well as an inducible, acinar-specific, AT-1 knockout mouse model to probe the effects of AT-1 function on pancreatic outcomes. We found that loss of AT-1 activity in pancreas leads to persistent UPR activation, inflammation, and fibrosis consistent with a mild/moderate CP-like phenotype that includes increased trypsin activation. Furthermore, we found that AT-1 expression is decreased in experimental models of both AP and CP. These results suggest that AT-1, and thus ER acetyl-CoA availability, plays an important role in pancreatic acinar cell protein maturation and that loss of AT-1 is a previously unrecognized event in the pathology of pancreatitis.

## Results

### *Relationship of AT-1 Expression, ER Stress, and Pancreatitis*

The AT-1 (gene *SLC33A1*) was shown to be down-regulated in gene expression analyses of rat pancreas subject to alcohol-induced injury, however, AT-1 expression during pancreatitis has not been investigated previously.<sup>23</sup> Here, we show that AT-1 mRNA is reduced by greater than 50% after in vivo cerulein (CER)-induced AP in C57BL/6 wild-type (WT) mice (Figure 1A), while AT-1 mRNA was decreased in 75% of WT mice subject to CER CP (Figure 1B). To determine the response at the initiation of pancreatitis, we isolated WT mouse acini and stimulated them with cholecystokinin (CCK)-8 at basal (0 pmol/L), physiological (3 pmol/L), and superphysiological (100 nmol/L) levels for 90 minutes, the latter of which induces in vitro pancreatitis; AT-1 mRNA expression increased significantly with superphysiological stimulation compared with basal (Figure 1C). Taken together, these data show that AT-1 is up-regulated at the onset of pancreatitis, and decreases as the disease progresses, under both acute and chronic conditions.

Given the critical role of AT-1 in maintaining ER proteostasis and the well-defined relationship of increased ER

**Abbreviations used in this paper:** AP, acute pancreatitis; AT-1, acetyl-CoA transporter 1 *SLC33A1*; ATF, activating transcription factor; CCK, cholecystokinin; cDNA, complementary DNA; CER, cerulein; CHOP, CCAAT/enhancer-binding protein homologous protein; CP, chronic pancreatitis; eIF2 $\alpha$ , elongation initiation factor 2 $\alpha$ ; ER, endoplasmic reticulum; IRE1, inositol-requiring enzyme 1; KO, knockout; mRNA, messenger RNA; PBS, phosphate-buffered saline; PERK, protein kinase R-like ER kinase; qPCR, quantitative polymerase chain reaction; Tm, tamoxifen; UPR, unfolded protein response; WT, wild-type; XBP1, x-box binding protein 1; XBP1s, x-box binding protein 1 spliced.

 Most current article

© 2020 The Authors. Published by Elsevier Inc. on behalf of the AGA Institute. This is an open access article under the CC BY-NC-ND license (<http://creativecommons.org/licenses/by-nc-nd/4.0/>).

2352-345X

<https://doi.org/10.1016/j.jcmgh.2020.10.008>

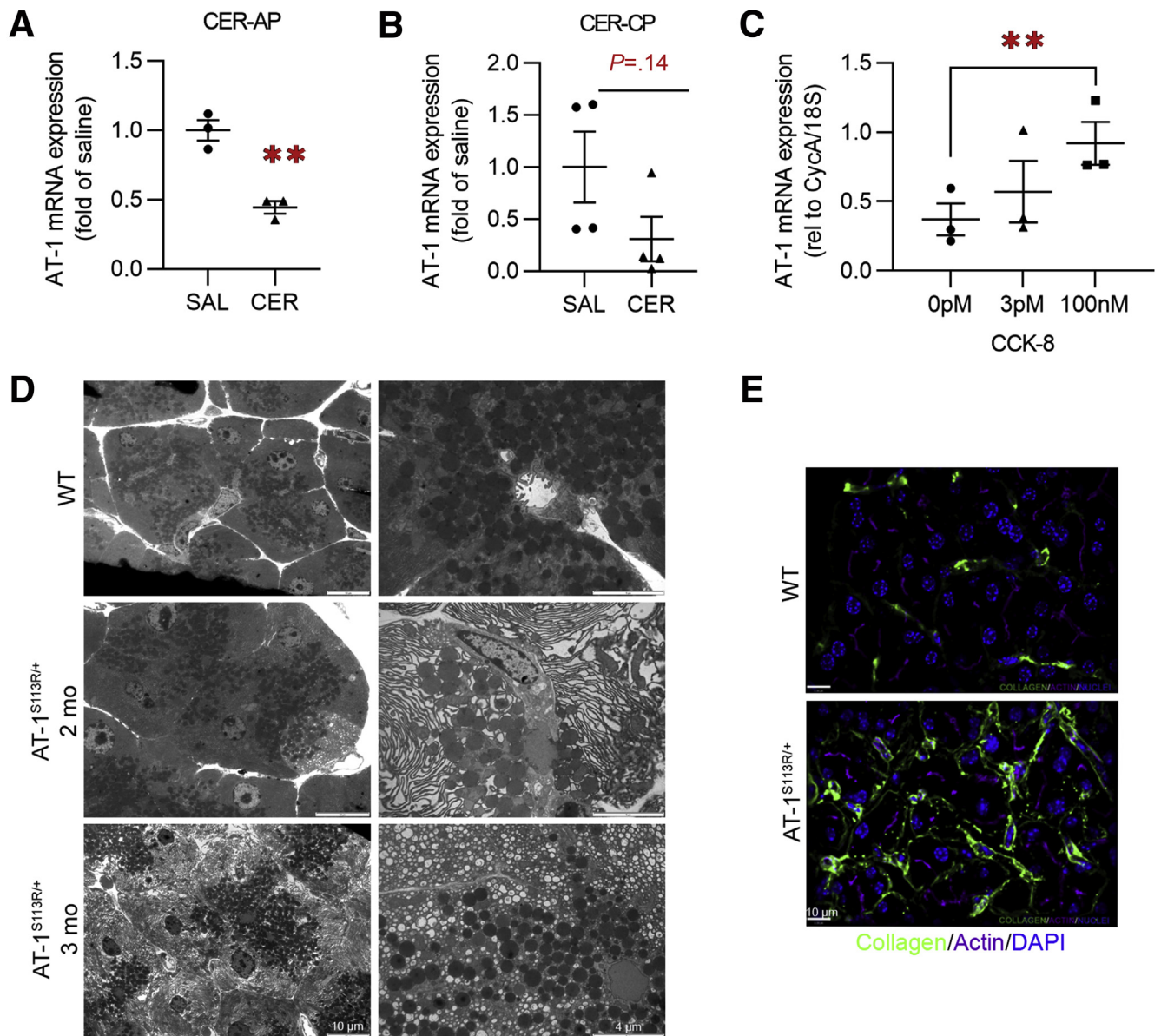


**Figure 1. AT-1 reduction is associated with pancreatitis.** AT-1 mRNA expression in pancreas from C57BL/6 WT mice treated with saline (SAL) or CER to (A) induce AP or (B) CP. (C) AT-1 mRNA expression in WT mouse acini treated with 0 pmol/L, 3 pmol/L (physiological), or 100 nmol/L (superphysiological) CCK-8. (D) Electron microscopy of pancreatic tissue from WT and hypomorphic AT-1<sup>S113R/+</sup> pancreas at 2 and 4 months of age. (E) Immunofluorescence of type 1 collagen (green) and actin (purple) in WT and AT-1<sup>S113R/+</sup> pancreatic sections. Data are means  $\pm$  SE,  $n = 3-5$ . \*\* $P < .01$ . Statistical comparison of means was performed by (A and B) unpaired 2-tailed Student  $t$  test or (C) 1-way analysis of variance. DAPI, 4',6-diamidino-2-phenylindole.

stress and pancreatitis, we examined whether dysregulation of AT-1 function itself would be sufficient to induce pancreatitis. AT-1<sup>S113R/+</sup> mice, which express a heterozygous hypomorphic mutation that prevents AT-1 dimerization, have an approximate 50% reduction in ER acetyl-CoA transport activity.<sup>20</sup> Notwithstanding the immune dysfunction reported in these mice, AT-1<sup>S113R/+</sup> acinar cells show widespread ER dilation and accumulation of intracellular vacuoles, indicative of ER stress and cellular damage, which progresses with age (Figure 1D). Likewise, AT-1<sup>S113R/+</sup> pancreas have increased collagen deposition (Figure 1E), a marker of fibrosis. Altogether, these data suggest a 2-way

relationship between pancreatic injury and AT-1 expression/function, and changes in AT-1 regulation are a previously unknown occurrence in pancreatitis pathology.

#### Generation of Acinar-Specific AT-1 Knockout (KO) Mice

To circumvent the immune dysfunction in the global AT-1<sup>S113R/+</sup> model, we crossed AT-1 floxed (Slc33a1<sup>tm1a[KOMP]Wtsi</sup>) mice with mice expressing tamoxifen (Tm)-inducible Cre driven by the acinar-specific elastase promoter (Tg[Cela1-cre/ERT]1Lgdn/Jd<sup>24</sup>) to produce cell-specific heterozygous

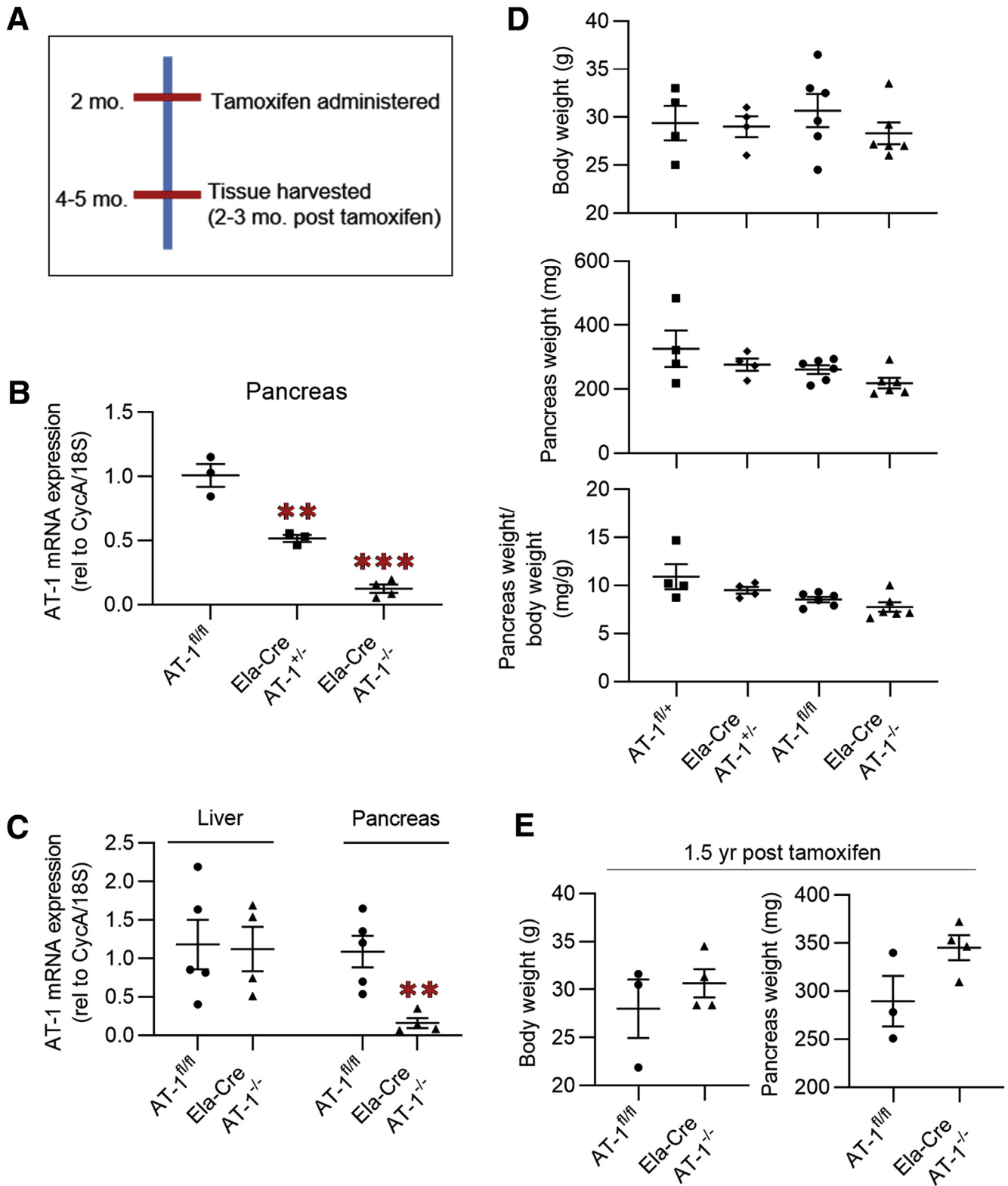


**Figure 2. Characterization of tamoxifen-inducible, acinar-specific AT-1 mice.** (A) Schematic of Ela-Cre AT-1 mouse production. KO was induced by Tm at 2 months of age to allow for normal pancreatic development; tissues were analyzed 2–3 months afterward. Controls also received Tm. (B and C) AT-1 mRNA levels in whole pancreas and/or liver from AT-1<sup>fl/fl</sup>, Ela-Cre AT-1<sup>+/-</sup>, and Ela-Cre AT-1<sup>-/-</sup> mice, as indicated. (D and E) Measurement of body weight, pancreas weight, and pancreas weight normalized to body weight between AT-1<sup>fl/fl</sup>, Ela-Cre AT-1<sup>+/-</sup>, AT-1<sup>fl/fl</sup>, and Ela-Cre AT-1<sup>-/-</sup> mice at (D) 2–3 months after Tm or (E) 1.5 years after Tm. Data are means  $\pm$  SE,  $n = 3$ –5. \*\* $P < .01$ , \*\*\* $P < .001$ . Statistical comparison of means was performed by (C) unpaired 2-tailed Student  $t$  test or (B and D) 1-way analysis of variance. CycA, cyclophilin A.

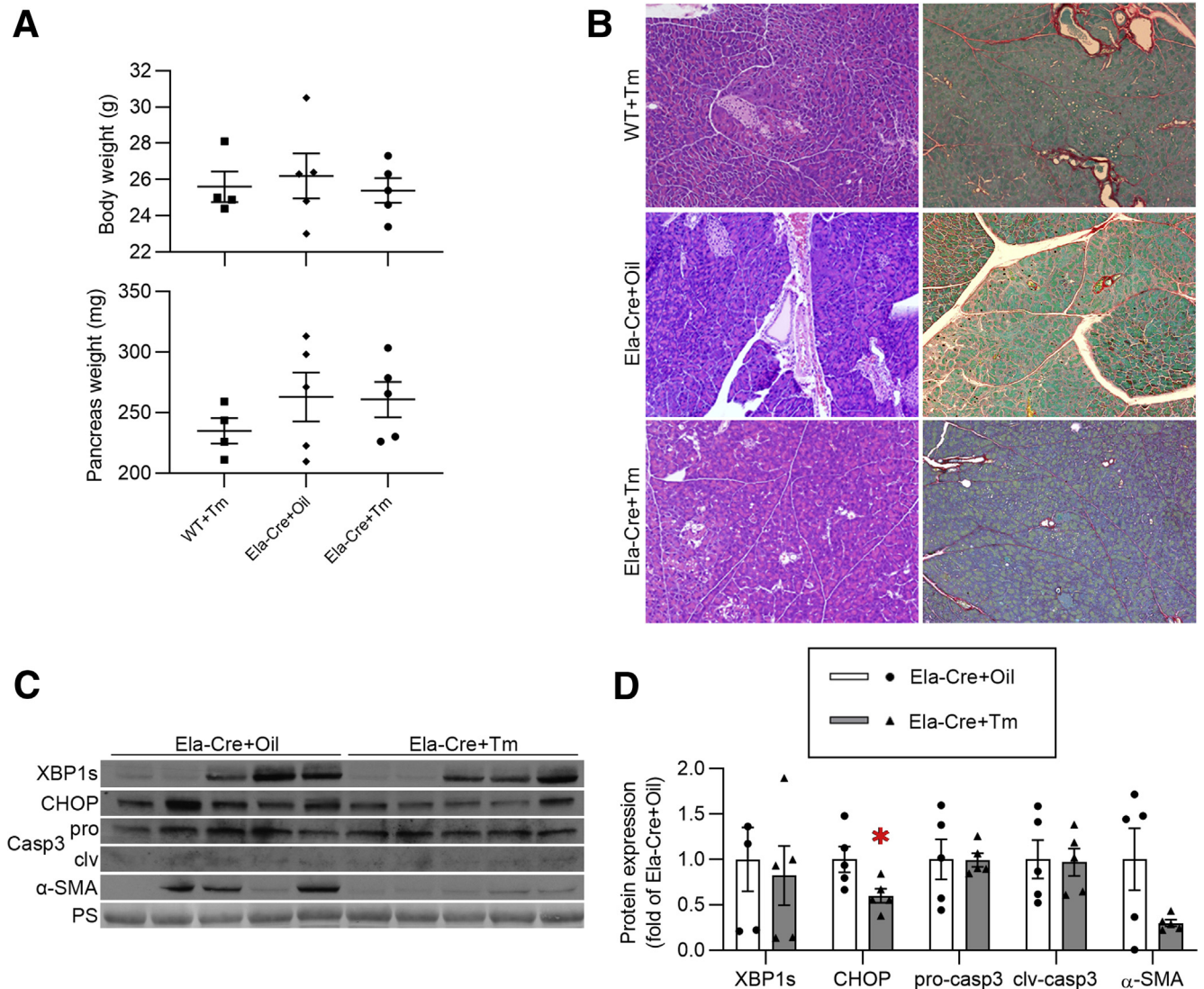


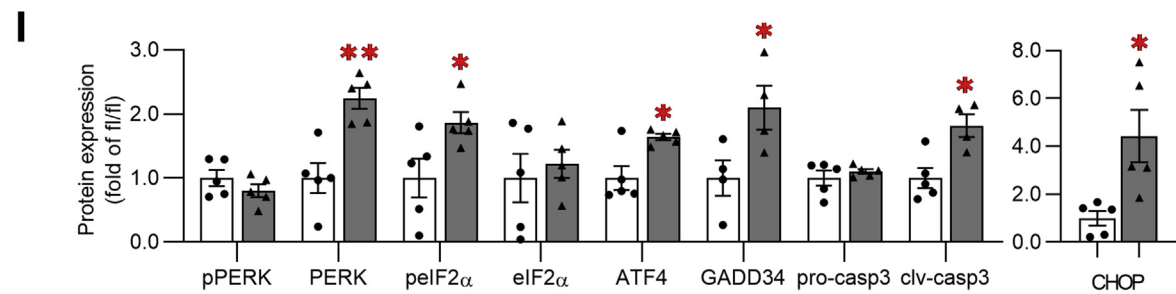
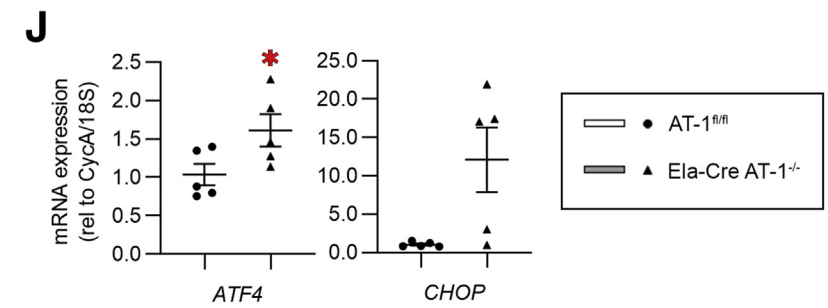
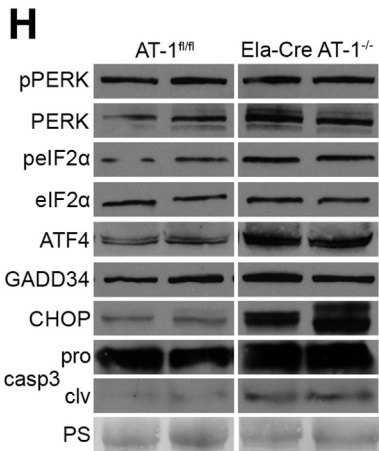
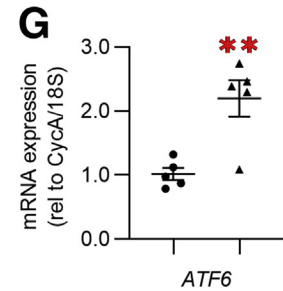
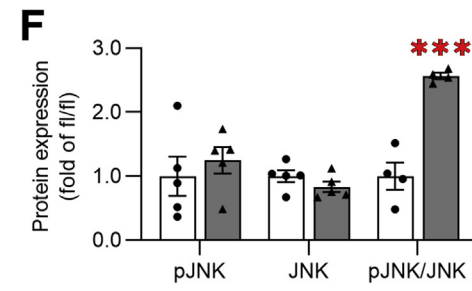
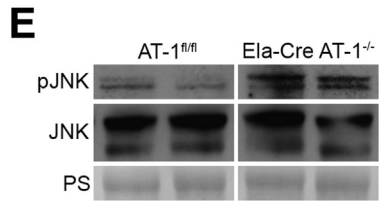
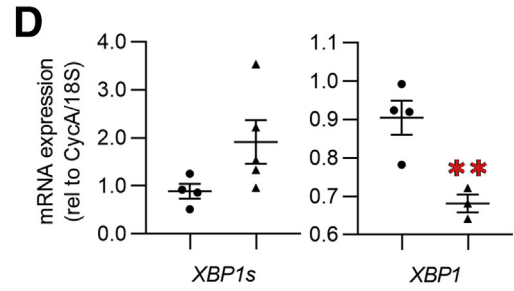
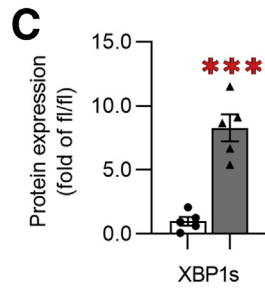
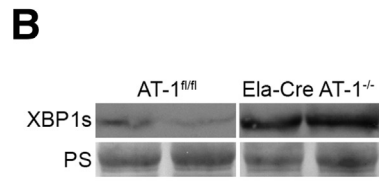
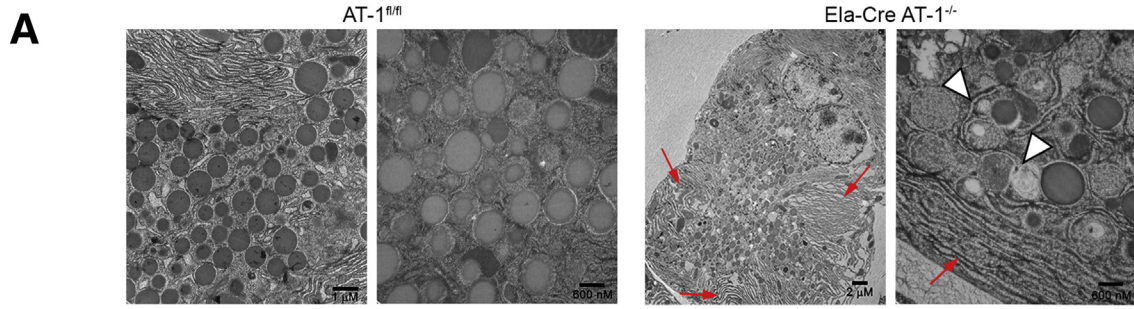
**Figure 3. Presence of tamoxifen or Cre expression does not produce a phenotype.** (A) Representative H&E and Sirius red staining of pancreas from WT or Ela-Cre mice given oil or Tm, as indicated. (B) Body weight and pancreatic weight. (C) Immunoblot of XBP1s, CHOP, caspase 3, and  $\alpha$ -smooth muscle actin ( $\alpha$ -SMA), quantified in panel D. Ponceau S (PS) was used as the loading control. Data are means  $\pm$  SE,  $n = 5$ . \* $P < .05$ . Statistical comparison of means was performed by unpaired 2-tailed Student  $t$  test. clv, cleaved caspase 3; pro, pro-caspase 3.

and homozygous AT-1 KO mice (Ela-Cre AT-1<sup>+/-</sup> and Ela-Cre AT-1<sup>-/-</sup>, respectively). To allow normal pancreas development, Tm was administered by oral gavage at 2 months of age and tissues were analyzed 2–3 months after Tm (Figure 2A). AT-1<sup>fl/fl</sup> control animals also received Tm. Pancreatic AT-1 mRNA was reduced by half in Ela-Cre AT-1<sup>+/-</sup> and approximately 90% loss in Ela-Cre AT-1<sup>-/-</sup> (Figure 2B), with no changes observed in liver (Figure 2C). Because AT-1 mRNA was measured from whole pancreatic tissue, residual AT-1 transcript expression in Ela-Cre AT-1<sup>-/-</sup> is from cells other than acini present in the mixed gland. No significant changes in body weight or pancreatic weight relative to body weight were observed at 4–5 months of age (Figure 2D) out to 1.5 years (Figure 2E). To eliminate possible toxicity resulting from Tm or the presence of Cre, we assessed weight, histology, and

biochemical parameters in WT or Ela-Cre mice given either Tm or oil alone; no overt differences were observed other than a modest reduction in CHOP in Ela-Cre+Tm, the reason for which is unclear (Figure 3).

### AT-1 Deletion Induces ER Stress

Electron microscopy of Ela-Cre AT-1<sup>-/-</sup> acini showed ER dilation and accumulation of vacuoles (Figure 4A), recapitulating the phenotype observed in AT-1<sup>S113R/+</sup> in Figure 1 (Figure 4A). Extensive UPR activation occurred marked by an 8-fold increase in XBP1s protein (Figure 4B and C) and a reduction in total XBP1 mRNA (Figure 4D). Furthermore, c-Jun N-terminal kinase activation was increased significantly in Ela-Cre AT-1<sup>-/-</sup>, likely owing to



web 4C/FPO

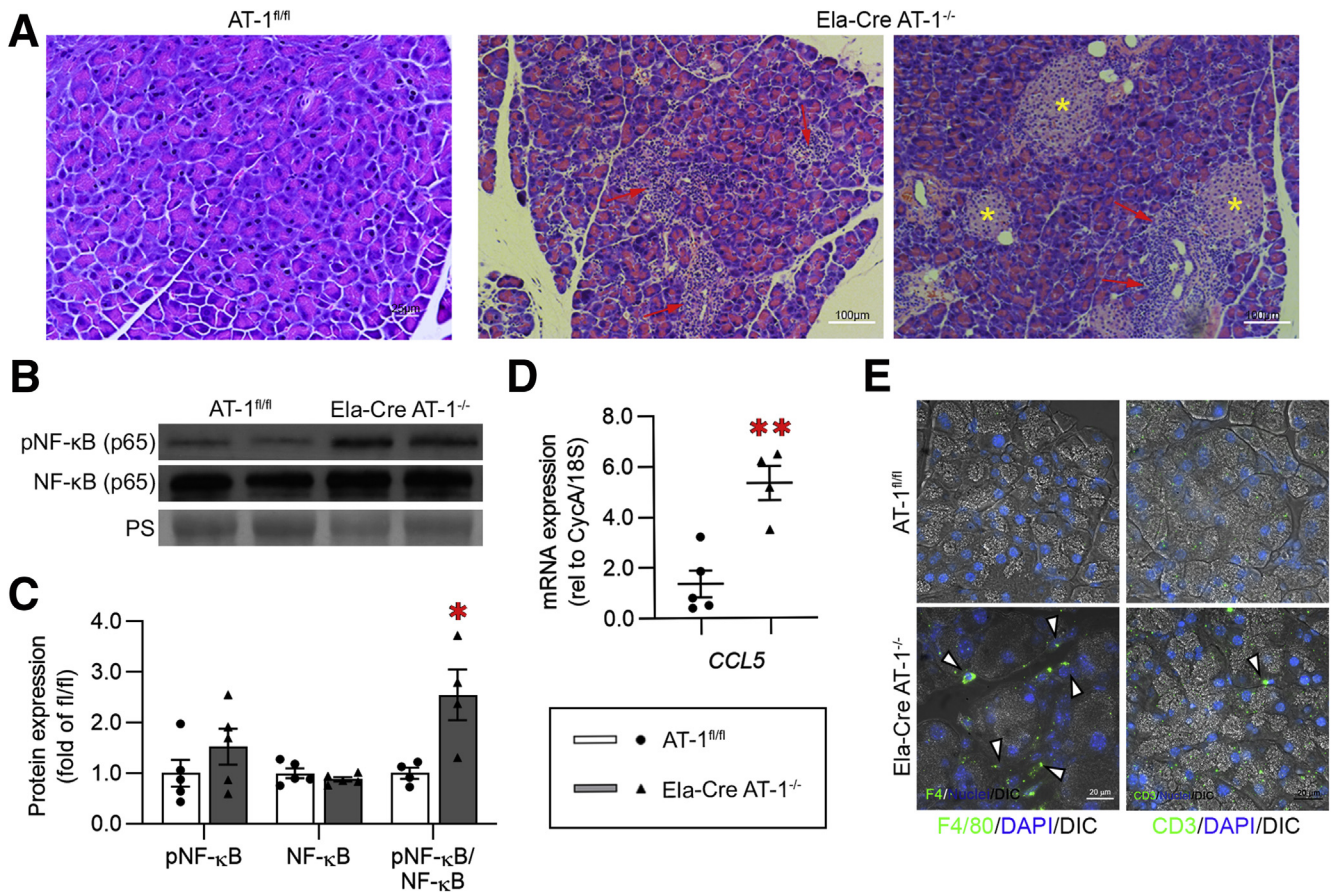


**Figure 5. Loss of AT-1 results in inflammation.** (A) Representative H&E staining of AT-1<sup>fl/fl</sup> and Ela-Cre AT-1<sup>-/-</sup> pancreatic sections. Note significant infiltration of immune cells in Ela-Cre AT-1<sup>-/-</sup> (red arrows). Islets are marked with yellow asterisks. (B) Immunoblot of phosphorylated and total nuclear factor-κB (NF-κB) (p65), quantified in panel C. Ponceau S (PS) was used as the loading control. (C) qPCR analysis of CCL5. (D) Representative IF images of immune cell markers F4/80 and CD3 (white arrowheads). Immunoblot and qPCR was performed in whole pancreas. All data are means ± SE, n = 4–5. \*P < .05, \*\*P < .01. Statistical comparison of means was performed by an unpaired 2-tailed Student t test. DAPI, 4',6-diamidino-2-phenylindole.

IRE1 hyperstimulation (Figure 4E and F).<sup>25–27</sup> ATF6 mRNA also was increased in Ela-Cre AT-1<sup>-/-</sup> compared with controls (Figure 4G). Finally, PERK and its downstream targets phosphorylates eIF2α, ATF4, growth arrest and DNA damage-inducible protein 34 (GADD34), and cell death mediators CHOP and cleaved caspase-3 all were increased significantly (Figure 4H, I, and J); notably, CHOP protein expression was increased 4-fold and mRNA expression increased approximately 10-fold (Figure 4I and J). Collectively, these results indicate that loss of ER acetyl-CoA availability via AT-1 deletion activates a pronounced response involving all known branches of the ER stress pathway.

#### *Ela-Cre AT-1<sup>-/-</sup> Pancreas Shows Inflammation and Fibrosis Consistent With CP*

Robust immune cell infiltration was evident by H&E staining in Ela-Cre AT-1<sup>-/-</sup> pancreas, a key pathologic event in pancreatitis (Figure 5A). Congruent with this observation, we found significant nuclear factor-κB activation (Figure 5B and C), and a 5-fold increase in expression of the potent chemokine C-C motif chemokine ligand 5 (Ccl5) (Figure 5D), a target of nuclear factor-κB. Immune cell species present in Ela-Cre AT-1<sup>-/-</sup> pancreas include predominantly F4/80<sup>+</sup> macrophages and, to a lesser extent, CD3<sup>+</sup> T cells (Figure 5E). Furthermore, Ela-Cre AT-1<sup>-/-</sup> pancreas showed significant α-smooth muscle actin up-regulation and collagen deposition by Sirius Red staining,

**Figure 4. (See previous page). Loss of AT-1 induces ER stress in pancreas.** (A) Representative electron microscopy images of pancreatic sections from AT-1<sup>fl/fl</sup> and Ela-Cre AT-1<sup>-/-</sup>. Red arrows indicate dilated ER; white arrowheads indicate vacuoles. (B) Immunoblot of sXBP1, quantified in panel C. (D) qPCR assessment of XBP1s, and XBP1 (tot) mRNA. (E) Immunoblot of phosphorylated c-jun N-terminal kinase (pJNK) and total c-jun N-terminal kinase (JNK), quantified in panel F. (G) qPCR of ATF6. (H) Immunoblot of phosphorylated PERK (pPERK), PERK, phosphorylates eIF2α (pEIF2α), eIF2α, ATF4, GADD34, caspase 3 (pro- and cleaved forms), and CHOP, quantified in panel I. (J) qPCR analysis of ATF4 and CHOP mRNA. Immunoblot and qPCR were performed in whole pancreas. Ponceau S (PS) is loading control. All data are means ± SE, n = 4–5. \*P < .05, \*\*P < .01, and \*\*\*P < .001. Statistical comparison of means was performed by an unpaired 2-tailed Student t test.

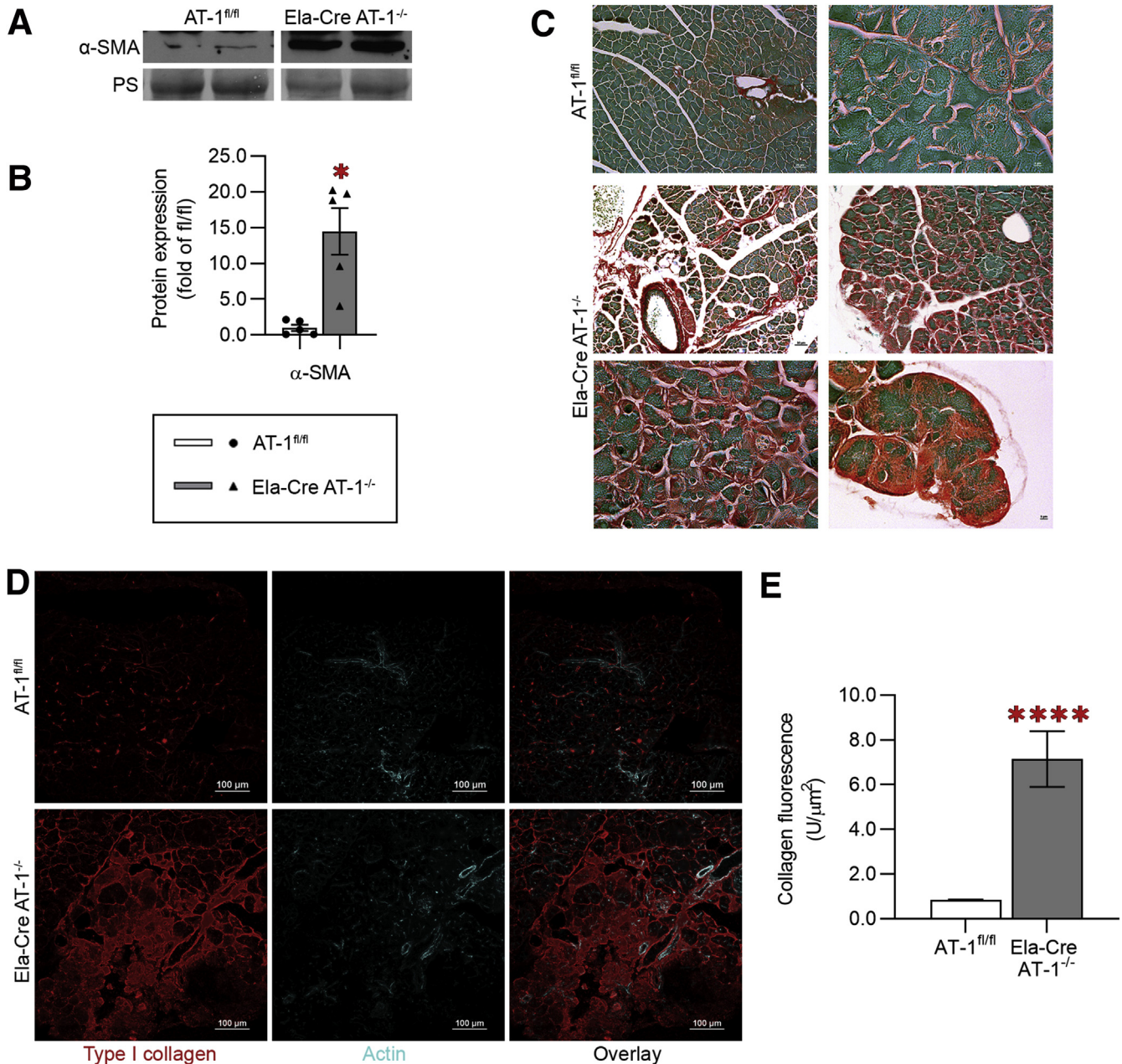


**Figure 6. AT-1 deletion induces fibrosis.** (A) Immunoblot of  $\alpha$ -smooth muscle actin ( $\alpha$ -SMA) in AT-1<sup>fl/fl</sup> and Ela-Cre AT-1<sup>-/-</sup> whole pancreas, quantified in panel B. Ponceau S (PS) was used as the loading control. (C) Representative Sirius red staining of AT-1<sup>fl/fl</sup> and Ela-Cre AT-1<sup>-/-</sup> pancreatic sections. (D) Representative IF images of type 1 collagen (red) and actin (blue), quantified in panel E. Data are means  $\pm$  SE, n = 4–5. \* $P < .05$ , \*\*\*\* $P < .0001$ . Statistical comparison of means was performed by an unpaired 2-tailed Student  $t$  test.

indicative of fibrosis (Figure 6A, B, and C). Indeed, Ela-Cre AT-1<sup>-/-</sup> pancreas had an 8-fold increase in collagen compared with controls (Figure 6D and E). Taken together, the presence of persistent UPR activation, chronic inflammation, and fibrosis support the presence of a CP-like phenotype with AT-1 deletion.

#### AT-1-Deficient CP Phenotype Includes Trypsin Activation

Unexpectedly, enhanced trypsin activity under basal conditions was detected in Ela-Cre AT-1<sup>-/-</sup> pancreas, a less

common phenomenon seen in CP vs AP (Figure 7A). Whether this activation is a consequence of decreased ER acetyl-CoA availability or pancreatic inflammation remains unknown. No differences in plasma amylase were observed (Figure 7B).

#### Acute-on-Chronic Pancreatitis Increases Disease Severity in Ela-Cre AT-1<sup>-/-</sup>

Despite the chronic ER stress, inflammation, and fibrosis, no pancreatic degeneration as noted by pancreatic weight

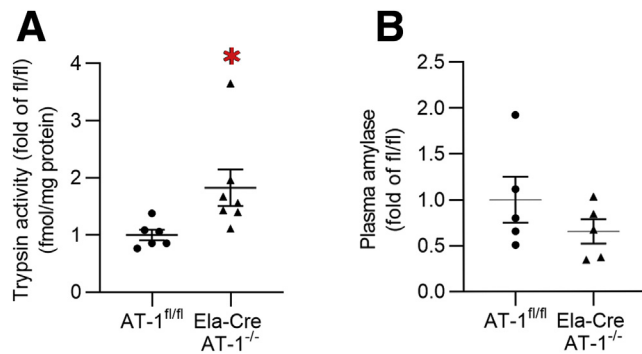


**Figure 7. Enzyme markers of CP.** (A) Measurement of trypsin activation. (B) Plasma amylase activity in AT-1<sup>fl/fl</sup> and Ela-Cre AT-1<sup>-/-</sup>. Data are means  $\pm$  SE,  $n \geq 3$ . \* $P < .05$ . Statistical comparison of means was performed by an unpaired 2-tailed Student  $t$  test.

was found with AT-1 deletion (Figure 2D), suggesting a mild/moderate CP phenotype. To examine the response to AP challenge, AT-1<sup>fl/fl</sup> and Ela-Cre AT-1<sup>-/-</sup> mice were subject to in vivo CER-AP for 2 consecutive days, and then analyzed after a 1-week recovery period (Figure 8A). Although AT-1<sup>fl/fl</sup> control mice showed pancreatic recovery, Ela-Cre AT-1<sup>-/-</sup> pancreas underwent significant atrophy with a 40% reduction in gland weight compared with controls, but no change in body weight (Figure 8B and C). This was confirmed by H&E staining showing extensive acinar cell loss and inflammatory cell infiltrates (Figure 8D). Together, these results support that inducing acute-on-chronic pancreatitis in Ela-Cre AT-1<sup>-/-</sup> results in a severe CP phenotype.

## Discussion

Pathologic UPR activation is a key cellular event in AP development, and chronic UPR activity occurs in models of CP.<sup>3</sup> Here, we show that chronic ER stress induced by the loss of the ER acetyl-CoA transporter AT-1 in pancreatic acinar cells is sufficient to cause spontaneous mild/moderate CP. Deletion of AT-1 leads to broad and pronounced UPR up-regulation, inflammation, fibrosis, and, in response to CER-AP, significant gland atrophy and acinar cell loss.

Previous studies targeting ER stress regulatory molecules have shed light on their effects on pancreatic function and disease pathology and have uncovered a balance between protective (eg, IRE1/XBP1s) and pathologic (PERK/ATF4/CHOP) UPR in pancreatic physiology and disease.<sup>5,9,11,28</sup> The present study shows marked up-regulation and/or dysregulation of pathologic cellular pathways including PERK, CHOP, and c-jun N-terminal kinase with loss of AT-1; however, the CP observed in Ela-Cre AT-1<sup>-/-</sup> appeared to be relatively mild to moderate, suggesting a capability of acinar cells to adapt to chronic ER stress when the protective IRE1/XBP1s UPR is intact. Interestingly, it was shown previously that AT-1 expression may be downstream of IRE1/XBP1s, suggesting that AT-1 also may play a role in the protective ER stress response<sup>21</sup>; this is supported further by the finding that

AT-1 expression increases at the initiation of pancreatitis, but is down-regulated as the disease progresses. Furthermore, a recent study suggested that chronic ER stress induces a switch to eIF3-dependent translation, circumventing eIF2 $\alpha$  inhibition and partially restoring protein translation including that of ER functional proteins.<sup>29</sup> These compensatory mechanisms allow acini to continue functioning under high-stress conditions and may explain, in part, how, the AT-1 KO phenotype only progressed to severe CP with loss of pancreatic mass after repeated CER-AP. These results support the concept that the combination of environmental stressors and subclinical pathophysiological perturbations can supersede the adaptive capacity of the UPR in acinar cells and allow severe pancreatic damage to occur.

The effect of AT-1 deletion on pancreatic function contributes to a growing understanding of the significance of Nε-lysine acetylation in the ER on protein folding and ER stress responses.<sup>15–17</sup> Investigation of the ER acetylome in cultured cell models previously has identified proteins such as glucose-regulated protein 78 (aka immunoglobulin binding protein, BiP), lysosome-associated membrane protein 2, and cathepsin D as acetylation targets,<sup>30</sup> all of which are critical for pancreatic acinar cell function.<sup>31–34</sup> This calls into question the acetylation state of pancreatic acinar-specific proteins, including *PRSS1* and other digestive enzymes and regulatory molecules, and what the functional significance of these post-translational modifications might be on pancreatitis outcomes. Indeed, studies have shown increased UPR activity and CP-like outcomes in response to variants of *PRSS1* and *CPA1*, among others.<sup>35,36</sup> For example, the *CPA1* N256K mouse model shows a similar progressive CP phenotype as the AT-1 model, with increased XBP1s, CHOP, trypsin activation, fibrosis, and histologic damage.<sup>37</sup> A number of *PRSS1* mutants associated with pancreatitis also have been investigated, including but not limited to p.R116C, p.C139S, p.L10P, p.22G, and p.K23R.<sup>35</sup> These mutants are presumed to be misfolded because they are poorly secreted when expressed in cultured cell models and prompt UPR signaling to various degrees. We posit that some of these mutations, especially those involving lysines and acetyl-like residues (eg, Q and R), could alternatively alter their acetylation state and thus affect their ability to traverse through the secretory pathway. Further investigation into the pancreatic acinar cell ER acetylome will be necessary to show additional insights.

In conclusion, this study identifies a previously unrecognized role of the ER acetyl-CoA transporter AT-1 in pancreatic acinar cell function and homeostasis, and uncovers a new layer of complexity of the pathologic ER stress response and its impact on pancreatic disease.

## Methods

All authors had access to the study data and reviewed and approved the final manuscript.

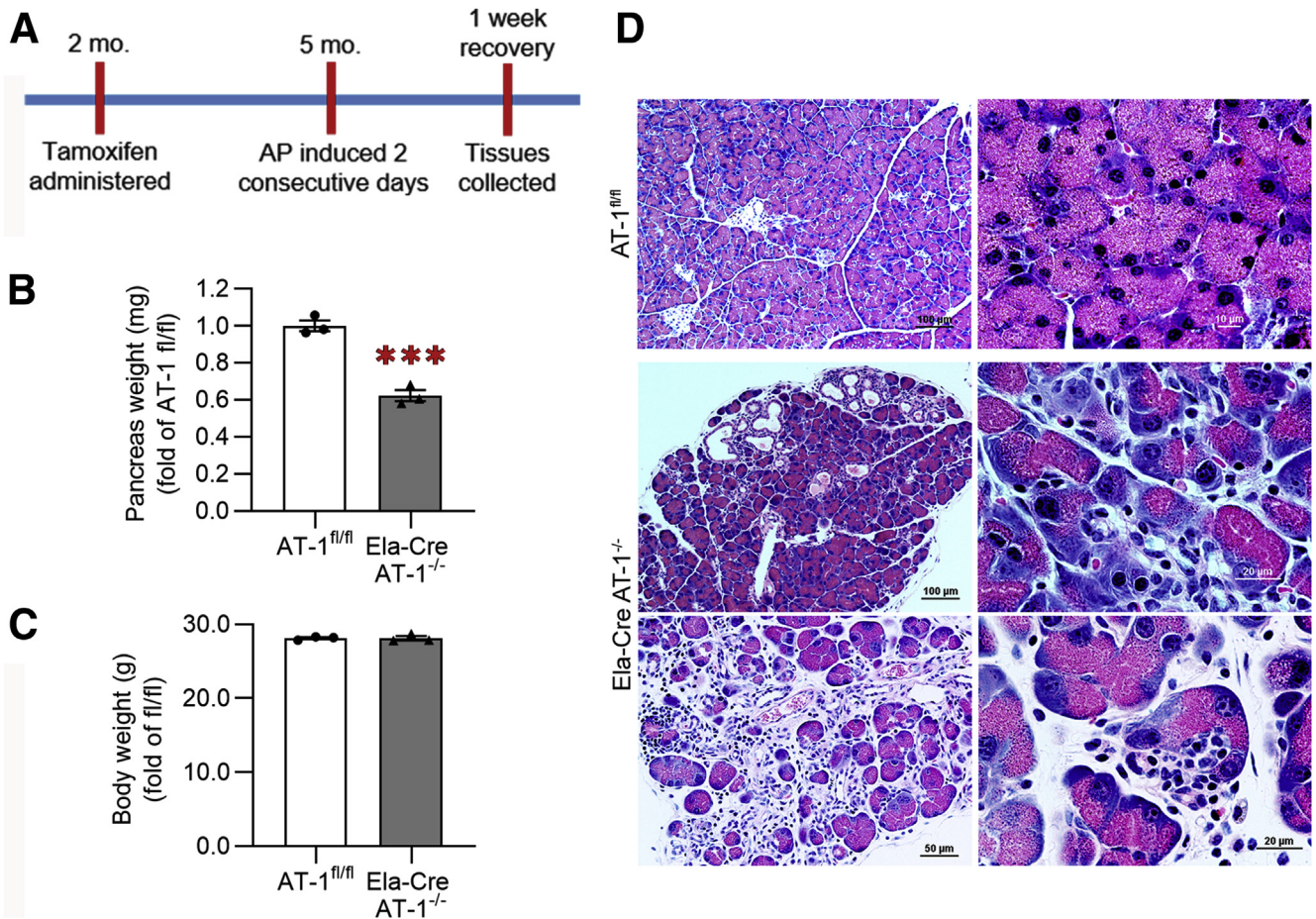


**Figure 8. Ela-Cre AT-1<sup>-/-</sup> sustain significant damage during AP.** (A) Experimental schematic: AT-1<sup>fl/fl</sup> and Ela-Cre AT-1<sup>-/-</sup> mice given CER AP and allowed to recover for 1 week. (B) Pancreatic weight and (C) body weight after the experiment. (D) Representative H&E staining of AT-1<sup>fl/fl</sup> and Ela-Cre AT-1<sup>-/-</sup> pancreatic sections. Data are means  $\pm$  SE,  $n = 3$ . \*\*\* $P < .001$ . Statistical comparison of means was performed by an unpaired 2-tailed Student  $t$  test.

### Reagents

**Antibodies.** Antibodies used for immunoblotting and/or immunofluorescence and their source are indicated in Table 1. Peroxidase-conjugated secondary antibodies were from GE Healthcare (Pittsburgh, PA). Alexa-conjugated secondary antibodies were from Invitrogen/Life Technologies (Carlsbad, CA).

**Quantitative polymerase chain reaction primers.** Quantitative polymerase chain reaction (qPCR) primers were designed using NCBI Primer Blast (Bethesda, MD) unless otherwise indicated (Table 2).

### Mouse Studies

**Production of tamoxifen-inducible, acinar-specific AT-1 KO mice.** Slc33a1<sup>tm1a(KOMP)Wtsi</sup> heterozygous mice (C57BL/6N background; design ID: 44962; project ID: CSD28391) were purchased from the University of California–Davis Knockout Mouse Project Repository and bred with transgenic mice expressing flippase recombinase (CAG-Flpo1Afst/Mmucd heterozygous, C57BL6/N background) to remove the targeting cassette to produce AT-1<sup>fl/+</sup> mice. These mice then were crossed together and

offspring without Flpo expression were used to propagate the colony. Subsequent AT-1<sup>fl/+</sup> or AT-1<sup>fl/fl</sup> mice then were crossed with transgenic mice expressing a tamoxifen-inducible Cre recombinase driven by the acinar-specific elastase promoter (Tg[Cela1-cre/ERT]1Lgdn/J, C57BL/6 background, gifted by Drs Craig Logsdon and Baoan Ji).<sup>24</sup> About 50% Cre activity in the absence of tamoxifen has been shown in this elastase Cre model after 2 months; significantly, however, administration of tamoxifen induces Cre activity with 100% efficiency, which remains stable for 2 years.<sup>24</sup> The number of animals used in each experiment is shown in the figure legends of Figures 1-7. Experimental numbers may vary because not all mice were analyzed for all parameters. Only male mice were studied because we have identified inflammatory persistence in female mice with tamoxifen treatment.

Ela-Cre AT-1<sup>fl/+</sup> and Ela-Cre AT-1<sup>fl/fl</sup> mice at 2-3 months of age were treated with tamoxifen (MP Bio-medicals [Solon, OH], 3 mg/40 g body weight dissolved in 98% corn oil [Sigma, St. Louis, MO] and 2% ethanol [Sigma]) by oral gavage once daily for 3 days to induce Cre recombinase activity. AT-1<sup>fl/+</sup> and AT-1<sup>fl/fl</sup> mice were used

**Table 1.** Primary Antibodies

Target	Source	Cat.
Actin	AbCam (Cambridge, UK)	Ab6276
Amylase	Sigma-Aldrich (St. Louis, MO)	A8273
ATF4	Santa Cruz (Dallas, TX)	sc-200
Caspase 3	Thermo Fisher (Waltham, MA)	PA5-16385
CD3	AbCam	Ab16669
CD45R	AbCam	Ab64100
CHOP	Cell Signaling (Danvers, MA)	cs-2895
Collagen, type 1	Thermo Fisher	PA5-29569
eIF2 $\alpha$	Cell Signaling	cs-9722
p-eIF2 $\alpha$	Cell Signaling	cs-9721
F4/80	AbCam	Ab6640
GADD34	Santa Cruz	sc-8327
JNK	Cell Signaling	cs-9252
p-JNK	Cell Signaling	cs-4668
Lipase	Cortex Biochem (Leandro, CA)	CR8018M1
NF- $\kappa$ B	Cell Signaling	cs-8242
p-NF- $\kappa$ B	Cell Signaling	cs-3033
PERK	Cell Signaling	cs-3192
pPERK	Santa Cruz	sc-32577
Smooth muscle actin	Sigma-Aldrich	A7607
XBP1	Santa Cruz	sc-7160

p-JNK, phosphorylated c-jun N-terminal kinase; p-NF- $\kappa$ B, phosphorylated nuclear factor- $\kappa$ B; p-eIF2 $\alpha$ , phosphorylated elongation initiation factor 2 $\alpha$

as controls. Tissues were harvested at the indicated time points and analyzed as described later.

*In vivo pancreatitis.* C57BL/6 WT mice were given intraperitoneal injections of either saline or cerulein (50  $\mu$ g/kg body weight; MP Biomedicals) to induce pancreatitis

(Figure 1). For AP, mice were given 7 injections, 1 injection each hour for 7 hours; tissues were collected 1 hour after the last injection. For CP, mice received 7 hourly injections 3 days per week for a total of 4 weeks; tissues were collected 4 days after the last day of injections. To induce AP in AT-1<sup>fl/fl</sup> and

**Table 2.** Primers for qPCR

Target	Forward primer sequence	Reverse primer sequence	Source
18S	GTAACCCGTTGAACCCATT	CCATCCAATCGGTAGTAGCG	
AT-1 (Slc33A1)	GGAATCGTTACCCTTTCAGATTT	GATCCCTTGGGTCTCTTCTTT	Dr Luigi Puglielli
ATF4	CCTATAAAGGCTTGCGGCCA	GTCCGTTACAGCAACTGTC	
ATF6	TCGTGTTCTCAACTCAGCAC	TGGAGTCAGTCCATGTTCTGT	Dr Feyza Engin
Ccl5	CCTCACCATATGGCTCGGAC	ACGACTGCAAGATTGGAGCA	
CHOP	ACCTGAGGAGAGAGTGTCCA	CAAGGTGAAAGGCAGGGACT	L. Antonucci, J.B. Fagman, J.Y. Kim, J. Todoric, I. Gukovsky, M. Mackey, M.H. Ellisman and M. Karin. Basal autophagy maintains pancreatic acinar cell homeostasis and protein synthesis and prevents ERstress, PNAS, 112, 2015, 6166-6174.
Cyclophilin A	CTGCCAAGACTGAATGGCTG	CCCAAACGCTCCATGGCTT	
XBP1s	CTGAGTCCGAATCAGGTGCAG	GTCCATGGGAAGATGTTCTGG	X. Zhu, F. Yao, Y. Yao, N. Dong, Y. Yu and Z. Sheng. Endoplasmic reticulum stress and its regulator XBP-1 contributes to dendritic cell maturation and activation induced by high mobility group box-1 protein, Int J Biochem Cell Biol, 44, 2012, 1097-1105.
XBP1(tot)	TGCCCGGTCTGCTGAGTCCG	GTCCATGGGAAGATGTTCTGG	Zhu et al, 2012; JBC

Ela-Cre AT-1<sup>-/-</sup> mice were given 7 intraperitoneal injections of cerulein (50  $\mu\text{g}/\text{kg}$  body weight; MP Biomedicals), 1 injection each hour for 7 hours, for 2 consecutive days (Figure 7). To assess pancreatitis recovery, mice were harvested 7 days after pancreatitis induction.

### Trypsin Activity Assay

Trypsin activity was measured in homogenates of pancreatic acini by a fluorogenic assay as previously reported.<sup>32</sup> Briefly, the tissue was homogenized in a buffer containing 5 mmol/L 2-(N-morpholino)ethanesulfonic acid, 1 mmol/L  $\text{MgSO}_4$ , and 250 mmol/L sucrose (pH 6.5). An aliquot of the homogenate (100–200  $\mu\text{g}$  protein) was incubated at 37°C for 300 seconds in assay buffer containing 50 mmol/L Tris (pH 8.0), 150 mmol/L NaCl, 1 mmol/L  $\text{CaCl}_2$ , and 0.1 mg/mL bovine serum albumin and Boc-Gln-Ala-Arg-7-amino-4-methylcoumarin as a specific substrate for trypsin. Cleavage of this substrate by trypsin releases 7-amino-4-methylcoumarin, which emits fluorescence at 440 nm ( $\lambda_{\text{em}}$ ), with excitation at 380 nm ( $\lambda_{\text{ex}}$ ). Trypsin activity in each sample was determined using a standard curve for purified trypsin (Sigma).

### Plasma Amylase Assay

Plasma was prepared by centrifuging mixed arteriovenous blood from each mouse at  $3000 \times g$  for 15 minutes at 4°C. Plasma amylase activity then was determined using the Phadebas Amylase Assay tablets (Magle Life Sciences, Lund, Sweden).

### Immunoblotting

Pancreatic tissue harvested from mice was homogenized in a Tris-base buffer containing TritonX-100 detergent (0.2%; Sigma) and supplemented with benzamidine (1 mmol/L; Sigma), soybean trypsin inhibitor (0.1 mg/mL; Gibco, Grand Island, NY), phenylmethanesulfonylfluoride fluoride (1 mmol/L; Sigma), and protease inhibitor cocktail (1%; Calbiochem, San Diego, CA). Tissue was homogenized using a Tissue Tearor (BioSpec Products, Bartlesville, OK) followed by centrifugation at  $1000 \times g$  at 4°C for 10 minutes to clear cellular debris. The protein concentration of the supernatant was determined using BioRad (Hercules, CA) Protein Assay Dye Reagent Concentrate. Sodium dodecyl sulfate–polyacrylamide gel electrophoresis and immunoblot analyses were performed as previously described.<sup>39</sup> Membranes were stained with Ponceau S solution (Sigma) to assess the relative total protein load per lane as loading controls. Antibody information is provided in Table 1.

### qPCR

Harvested pancreatic tissue was stored in RNeasy RNA Stabilization Reagent (Qiagen, Hilden, Germany) for later RNA extraction. RNA was extracted from pancreatic tissue using the Qiagen RNeasy Plus Mini Kit, starting with approximately 15 mg of tissue that was homogenized in RLT buffer using a Tissue Tearor (BioSpec Products, Bartlesville, OK). The concentration and purity of the RNA was assessed using Nanodrop (Thermo Fisher, Waltham, MA) and agarose gel analyses. RNA then was used for complementary DNA

(cDNA) synthesis using the iScript cDNA synthesis kit (BioRad, Hercules, CA). cDNA templates were used for real-time qPCR with the KAPA SYBR Fast qPCR kit (KAPA Biosystems/Roche, Basel, Switzerland) and analyzed with the Roche LightCycler 480. Relative transcript levels were calculated using the  $2^{-\Delta\Delta\text{Ct}}$  (delta delta cycle threshold) method, using the geometric mean of cyclophilin A (CycA) and 18S as internal controls as previously described.<sup>40</sup> Primer pairs are provided in Table 2.

### H&E Staining

Pancreatic lobules were fixed in 4% paraformaldehyde (Ted Pella, Redding, CA) overnight, then washed with phosphate-buffered saline (PBS) and placed in 70% ethanol (Sigma). Samples were embedded in paraffin and processed for H&E at the Translational Research Initiatives in Pathology (TRIP) Laboratory facility at the University of Wisconsin.

### Picro Sirius Red and Fast Green Staining

Standard deparaffination of tissue was followed by 2 minutes in 0.2% phosphomolybdic acid (Thermo Fisher), brief rinsing in distilled water, and then 15 minutes in 0.1% Fast Green (Fisher) dissolved in saturated picric acid (Thermo Fisher). Slides then were rinsed in distilled water and placed in 0.1% Fast Green dissolved in Picro Sirius Red F3BA solution (VWR, Radnor, PA) for 1 hour, then rinsed in 0.1 N HCl for 2 minutes, followed by brief rinses in 70%, 95%, 100% ethanol and, finally, 5 minutes in xylene (Thermo Fisher) (in that order). Slides then were mounted with coverslips using solvent-based mounting media.

### High-Pressure Freezing Electron Microscopy

In vivo animal fixation was used according to an approved animal protocol. Animals were anesthetized; a mixed solution of 2% formaldehyde (Ted Pella, Redding, CA) and 2% glutaraldehyde (Electron Microscopy Sciences) in  $1 \times$  Sorensen's PB (Electron Microscopy Sciences, Hatfield, PA) was allowed to perfuse briefly into the animals' circulatory system via the heart. Next, the pancreas was removed, trimmed, and allowed to fix overnight in 2% formaldehyde/2% glutaraldehyde. Tissue then was dissected into 1 mm  $\times$  1 mm pieces, rinsed well with 0.1 mol/L PB, dipped in 20% bovine serum albumin in filtered water, placed on planchets coated with hexadecane (Ted Pella), and introduced into the high pressure freezing machine. Samples next underwent freeze substitution and dehydration over 2 days in 2% osmium tetroxide (Electron Microscopy Sciences, Hatfield, PA) and acetone (Thermo Fisher) with liquid nitrogen. Samples then were embedded in Epon, sectioned, and processed as previously described for imaging.<sup>41</sup>

### Immunofluorescence Microscopy

Immunofluorescence microscopy was conducted on cryostat sections of 4% paraformaldehyde fixed pancreatic lobules as previously described.<sup>42</sup> Blocking and incubations were performed in PBS supplemented with 3% bovine serum albumin (Calbiochem; San Diego, CA); 2% goat serum

(Sigma); 0.7% cold-water, fish-skin gelatin (Sigma); and 0.2% Triton X-100 (Sigma). Cryostat sections were rinsed with PBS and then treated with Image-iT FX (Invitrogen/Life Technologies) according to the manufacturer's instructions. Primary antibodies were added simultaneously for 2 hours at room temperature. Sections were washed with PBS, and then incubated with secondary antibodies for 1 hour at room temperature. If indicated, tissue was incubated with Alexa-conjugated phalloidin (Invitrogen/Life Technologies) to label actin according to the manufacturer's instructions. Sections were washed again with PBS and mounted with coverslips and ProLong Gold antifade reagent with 4',6-diamidino-2-phenylindole (Invitrogen/Life Technologies) to label nuclei.

### Acinar Cell Isolation and CCK Stimulation

Pancreatic acini were isolated from mouse pancreatic tissue by collagenase digestion as previously described.<sup>43</sup> Acini were incubated in salt-balanced HEPES buffer with or without CCK-8 (Research Plus; Farmingdale, NJ), as indicated, at 37°C for 90 minutes. Cells were collected and lysed immediately for RNA extraction, cDNA preparation, and subject to qPCR analysis as described earlier.

### Statistics

All data are expressed as means  $\pm$  SEM. Calculations were performed using GraphPad Prism 8.0 (GraphPad Software; San Diego, CA). A 2-tailed unpaired Student *t* test was used for comparison between 2 groups; F-tests were performed before *t* test analysis to determine equality of variance. One-way or 2-way analysis of variance was used for multiple group comparisons.

### References

1. Forsmark CE, Andersen DK, Farrar JT, Golden M, Habtezion A, Husain SZ, Li L, Mayerle J, Pandol SJ, Uc A, Zhu Z, Yadav D. Accelerating the drug delivery pipeline for acute and chronic pancreatitis: summary of the Working Group on Drug Development and Trials in Chronic Pancreatitis at the National Institute of Diabetes and Digestive and Kidney Diseases Workshop. *Pancreas* 2018;47:1200–1207.
2. Kubisch CH, Logsdon CD. Endoplasmic reticulum stress and the pancreatic acinar cell. *Expert Rev Gastroenterol Hepatol* 2008;2:249–260.
3. Sah RP, Garg SK, Dixit AK, Dudeja V, Dawra RK, Saluja AK. Endoplasmic reticulum stress is chronically activated in chronic pancreatitis. *J Biol Chem* 2014;289:27551–27561.
4. Waldron RT, Pandol S, Lugea A, Groblewski G. Endoplasmic reticulum stress and the unfolded protein response in exocrine pancreas physiology and pancreatitis, *Pancreapedia: Exocrine Pancreas Knowledge Base*, 2015, <https://doi.org/10.3998/panc.2015.41>.
5. Barrera K, Stanek A, Okochi K, Niewiadomska Z, Mueller C, Ou P, John D, Alfonso AE, Tenner S, Huan C. Acinar cell injury induced by inadequate unfolded protein response in acute pancreatitis. *World J Gastrointest Pathophysiol* 2018;9:37–46.
6. Gukovskaya AS, Gorelick FS, Groblewski GE, Mareninova OA, Lugea A, Antonucci L, Waldron RT, Habtezion A, Karin M, Pandol SJ, Gukovsky I. Recent insights into the pathogenic mechanism of pancreatitis: role of acinar cell organelle disorders. *Pancreas* 2019;48:459.
7. Lee A-H, Chu GC, Iwakoshi NN, Glimcher LH. XBP-1 is required for biogenesis of cellular secretory machinery of exocrine glands. *EMBO J* 2005;24:4368–4380.
8. Huh WJ, Esen E, Geahlen JH, Bredemeyer AJ, Lee A-H, Shi G, Konieczny SF, Glimcher LH, Mills JC. XBP1 controls maturation of gastric zymogenic cells by induction of MIST1 and expansion of the rough endoplasmic reticulum. *Gastroenterology* 2010;139:2038–2049.
9. Lugea A, Tischler D, Nguyen J, Gong J, Gukovsky I, French SW, Gorelick FS, Pandol SJ. Adaptive unfolded protein response attenuates alcohol-induced pancreatic damage. *Gastroenterology* 2011;140:987–997.
10. Lugea A, Gerloff A, Su H-Y, Xu Z, Go A, Hu C, French SW, Wilson JS, Apte MV, Waldron RT, Pandol SJ. The combination of alcohol and cigarette smoke induces endoplasmic reticulum stress and cell death in pancreatic acinar cells. *Gastroenterology* 2017;153:1674–1686.
11. Waldron RT, Su H-Y, Piplani H, Capri J, Cohn W, Whitelegge JP, Faull KF, Sakkiah S, Abrol R, Yang W, Zhou B, Freeman MR, Pandol SJ, Lugea A. Ethanol induced disordering of pancreatic acinar cell endoplasmic reticulum: an ER stress/defective unfolded protein response model. *Cell Mol Gastroenterol Hepatol* 2018;5:479–497.
12. Tabas I, Ron D. Integrating the mechanisms of apoptosis induced by endoplasmic reticulum stress. *Nat Cell Biol* 2011;13:184–190.
13. B'chir W, Maurin A-C, Carraro V, Averous J, Jousse C, Muranishi Y, Pary L, Stepien G, Fafourmoux P, Bruhat A. The eIF2 $\alpha$ /ATF4 pathway is essential for stress-induced autophagy gene expression. *Nucleic Acids Res* 2013;41:7683–7699.
14. Lugea A, Waldron RT, Mareninova OA, Shalbuva N, Deng N, Su H-Y, Thomas DD, Jones EK, Messenger SW, Yang J, Hu C, Gukovsky I, Liu Z, Groblewski GE, Gukovskaya AS, Gorelick FS, Pandol SJ. Human pancreatic acinar cells: proteomic characterization, physiologic responses, and organellar disorders in ex vivo pancreatitis. *Am J Pathol* 2017;187:2726–2743.
15. Pehar M, Puglielli L. Lysine acetylation in the lumen of the ER: a novel and essential function under the control of the UPR. *Biochim Biophys Acta* 2013;1833:686–697.
16. Peng Y, Puglielli L. N $\epsilon$ -lysine acetylation in the lumen of the endoplasmic reticulum: a way to regulate autophagy and maintain protein homeostasis in the secretory pathway. *Autophagy* 2016;12:1051–1052.
17. Farrugia MA, Puglielli L. N $\epsilon$ -lysine acetylation in the endoplasmic reticulum - a novel cellular mechanism that regulates proteostasis and autophagy. *J Cell Sci* 2018;131:jcs221747.
18. Ko MH, Puglielli L. Two endoplasmic reticulum (ER)/ER Golgi intermediate compartment-based lysine acetyltransferases post-translationally regulate BACE1 levels. *J Biol Chem* 2009;284:2482–2492.
19. Jonas MC, Pehar M, Puglielli L. AT-1 is the ER membrane acetyl-CoA transporter and is essential for cell viability. *J Cell Sci* 2010;123:3378–3388.

20. Peng Y, Li M, Clarkson BD, Pehar M, Lao PJ, Hillmer AT, Barnhart TE, Christian BT, Mitchell HA, Bendlin BB, Sandor M, Puglielli L. Deficient import of acetyl-CoA into the ER lumen causes neurodegeneration and propensity to infections, inflammation, and cancer. *J Neurosci* 2014; 34:6772–6789.
21. Pehar M, Jonas MC, Hare TM, Puglielli L. SLC33A1/AT-1 protein regulates the induction of autophagy downstream of IRE1/XBP1 pathway. *J Biol Chem* 2012; 287:29921–29930.
22. Romero R, Sánchez-Rivera FJ, Westcott PMK, Mercer KL, Bhutkar A, Muir A, González Robles TJ, Lamboy Rodríguez S, Liao LZ, Ng SR, Li L, Colón CI, Naranjo S, Beytagh MC, Lewis CA, Hsu PP, Bronson RT, Vander Heiden MG, Jacks T. Keap1 mutation renders lung adenocarcinomas dependent on Slc33a1. *Nat Cancer* 2020;1:589–602.
23. Kubisch CH, Gukovsky I, Lugea A, Pandol SJ, Kuick R, Misek DE, Hanash SM, Logsdon CD. Long-term ethanol consumption alters pancreatic gene expression in rats: a possible connection to pancreatic injury. *Pancreas* 2006; 33:68–76.
24. Ji B, Song J, Tsou L, Bi Y, Gaiser S, Mortensen R, Logsdon C. Robust acinar cell transgene expression of CreErT via BAC recombineering. *Genesis* 2008;46:390–395.
25. Urano F, Wang X, Bertolotti A, Zhang Y, Chung P, Harding HP, Ron D. Coupling of stress in the ER to activation of JNK protein kinases by transmembrane protein kinase IRE1. *Science* 2000;287:664–666.
26. Han D, Lerner AG, Vande Walle L, Upton J-P, Xu W, Hagen A, Backes BJ, Oakes SA, Papa FR. IRE1 $\alpha$  kinase activation modes control alternate endoribonuclease outputs to determine divergent cell fates. *Cell* 2009; 138:562–575.
27. Chen Y, Brandizzi F. IRE1: ER stress sensor and cell fate executor. *Trends Cell Biol* 2013;23:547–555.
28. Harding HP, Zeng H, Zhang Y, Jungries R, Chung P, Plesken H, Sabatini DD, Ron D. Diabetes mellitus and exocrine pancreatic dysfunction in Perk $-/-$  mice reveals a role for translational control in secretory cell survival. *Mol Cell* 2001;7:1153–1163.
29. Guan B-J, van Hoef V, Jobava R, Elroy-Stein O, Valasek LS, Cargnello M, Gao X-H, Krokowski D, Merrick WC, Kimball SR, Komar AA, Koromilas AE, Wynshaw-Boris A, Topisirovic I, Larsson O, Hatzoglou M. A unique ISR program determines cellular responses to chronic stress. *Mol Cell* 2017;68:885–900.e6.
30. Hegyi E, Sahin-Tóth M. Human CPA1 mutation causes digestive enzyme misfolding and chronic pancreatitis in mice. *Gut* 2019;68:301–312.
31. Sahin-Tóth M. Genetic risk in chronic pancreatitis: the misfolding-dependent pathway. *Curr Opin Gastroenterol* 2017;33:390–395.
32. Lugea A, Gong J, Nguyen J, Nieto J, French SW, Pandol SJ. Cholinergic mediation of alcohol-induced experimental pancreatitis: cholinergic effect on alcoholic pancreatitis. *Alcohol Clin Exp Res* 2010;34:1768–1781.
33. Kaspar KM, Thomas DDH, Taft WB, Takeshita E, Weng N, Groblewski GE. CaM kinase II regulation of CRHSP-28 phosphorylation in cultured mucosal T84 cells. *Am J Physiol Gastrointest Liver Physiol* 2003; 285:G1300–G1309.
34. Vandesompele J, De Preter K, Pattyn F, Poppe B, Van Roy N, De Paepe A, Speleman F. Accurate normalization of real-time quantitative RT-PCR data by geometric averaging of multiple internal control genes. *Genome Biol* 2002;3:34.1–34.11.
35. Messenger SW, Jones EK, Holthaus CL, Thomas DDH, Cooley MM, Byrne JA, Mareninova OA, Gukovskaya AS, Groblewski GE. Acute acinar pancreatitis blocks vesicle-associated membrane protein 8 (VAMP8)-dependent secretion, resulting in intracellular trypsin accumulation. *J Biol Chem* 2017; 292:7828–7839.
36. Messenger SW, Thomas DDH, Falkowski MA, Byrne JA, Gorelick FS, Groblewski GE. Tumor protein D52 controls trafficking of an apical endolysosomal secretory pathway in pancreatic acinar cells. *Am J Physiol Gastrointest Liver Physiol* 2013;305: G439–G452.
37. Williams JA. Isolation of rodent pancreatic acinar cells and acini by collagenase digestion. *Pancreapedia: Exocrine Pancreas Knowledge Base* 2010. <https://doi.org/10.3998/panc.2010.18>.

---

Received August 13, 2020. Accepted October 5, 2020.

#### Correspondence

Address correspondence to: Guy E. Groblewski, PhD, Department of Nutritional Sciences, University of Wisconsin-Madison, 1415 Linden Drive, Madison, Wisconsin 53706. e-mail: [grobey@nutrisci.wisc.edu](mailto:grobey@nutrisci.wisc.edu); fax: (313) 936-8813.

#### Acknowledgments

A previous version of this manuscript has been posted to the BioRxiv preprint server: bioRxiv 2020.03.25.008557; doi: <https://doi.org/10.1101/2020.03.25.008557>.

#### CRedit Authorship Contributions

Michelle M. Cooley (Conceptualization: Supporting; Data curation: Equal; Formal analysis: Lead; Methodology: Supporting; Validation: Supporting; Writing – original draft: Lead; Writing – review & editing: Lead);

Diana D.H. Thomas (Data curation: Equal; Methodology: Equal; Writing – original draft: Supporting; Writing – review & editing: Supporting);

Kali Deans (Data curation: Supporting; Formal analysis: Supporting; Methodology: Supporting; Writing – review & editing: Supporting); Yajing Peng (Data curation: Supporting);

Aurelia Lugea (Conceptualization: Supporting; Data curation: Supporting; Formal analysis: Supporting; Writing – original draft: Supporting; Writing – review & editing: Supporting);

Stephen J. Pandol (Conceptualization: Supporting; Funding acquisition: Supporting; Writing – original draft: Supporting; Writing – review & editing: Supporting);

Luigi Puglielli (Conceptualization: Equal; Formal analysis: Equal; Funding acquisition: Supporting; Writing – original draft: Supporting; Writing – review & editing: Supporting);

Guy E. Groblewski, PhD (Conceptualization: Equal; Formal analysis: Equal; Funding acquisition: Supporting; Writing – original draft: Supporting; Writing – review & editing: Supporting).

#### Conflicts of interest

The authors disclose no conflicts.

#### Funding

This work was supported by National Institutes of Health grants RO1DK07088 (G.E.G.), PO1DK098108 (G.E.G., A.L., and S.J.P.), RO1NS094154 (L.P.), RO1AG053937 (L.P.), RO1AG057408 (L.P.), and T32DK007665 (M.M.C.), and by United States Department of Agriculture/Hatch grant WIS01583 (G.E.G.).